

Absolute (γ, p_0) and (γ, p_1) cross sections and angular distributions for the light, deformed nucleus ^{19}F

E. Kerkhove, H. Ferdinande, R. Van de Vyver, P. Berkvens, P. Van Otten, E. Van Camp, and D. Ryckbosch
Laboratorium voor Kernfysika, Rijksuniversiteit Ghent, B-9000 Ghent, Belgium
 (Received 3 February 1984)

Absolute (γ, p_0) and (γ, p_1) differential cross sections for ^{19}F have been measured at seven angles in the energy interval between 13.4 and 25.8 MeV. A sum of Legendre polynomials was fitted to the angular distributions to deduce the angular distribution coefficients. The (γ, p_0) and (γ, p_1) cross sections have a similar magnitude and represent a minor fraction of the total photoproton channel. The global difference between the two cross sections is attributed to configurational splitting effects. From the (γ, p_0) angular distribution coefficients, an $E2$ cross section was estimated, contributing about 37% to the total $E2$ energy-weighted sum rule.

I. INTRODUCTION

Light $(2s-1d)$ shell nuclei have always received a great deal of attention in photonuclear physics. This is readily understandable, as these nuclei exhibit some very particular features, such as a great amount of fine structure in their photonuclear cross section, or a very large width of their giant dipole resonance (GDR). One of the reasons for this large width is believed to be the "configurational splitting" of the GDR in $(2s-1d)$ shell nuclei, due to the energy difference between excitations from various shells.

For some of these nuclei, the (γ, p_0) cross sections have been measured in great detail, using the inverse capture reaction.^{1,2} In the case of ^{19}F , this procedure could not be used, as the separation between the ground and first excited state in ^{19}F is extremely small. And yet, more information seems to be needed for light odd- Z nuclei in order to allow a detailed and systematic study of the effects leading to the observed small (γ, p_0) cross sections.³

The (γ, p_0) and (γ, p_1) differential cross sections at 90° have been measured only once for ^{19}F , by Tsubota *et al.*⁴ However, the energy resolution was rather poor, and no angular distribution measurements were performed. Detailed knowledge of the angular distribution would seem desirable in order to investigate the $E1$ - $E2$ interference effects on which the older (γ, p) results have revealed conflicting data,⁵⁻⁸ and to estimate the $E2$ contribution, if present, quantitatively.

A detailed study of the (γ, p_0) cross section for light, deformed nuclei is further hoped to lead to some specific information on the microscopic structure and the excitation mechanism of the giant resonances, not obtainable in spherical nuclei.⁹ To this end, Schmid and Do Dang have performed several theoretical calculations concerning the $^{19}\text{F}(p, \gamma_0)^{20}\text{Ne}$ cross section and angular distributions,⁹ and have compared their results with the experimental data.² Apart from the problem posed by the unpaired proton, such calculations would seem appropriate for the similarly deformed ^{19}F nucleus as well. To make such calculations useful, one should have at one's disposal detailed and reliable experimental results.

For all these reasons, we set up a careful and elaborate study of the $^{19}\text{F}(\gamma, p_0)$ and (γ, p_1) cross sections and angu-

lar distributions. On the other hand, it would be interesting to have more extensive (γ, n_0) measurements available, as the existing data¹⁰ cover too small an energy range to allow a detailed comparison with our (γ, p_0) result.

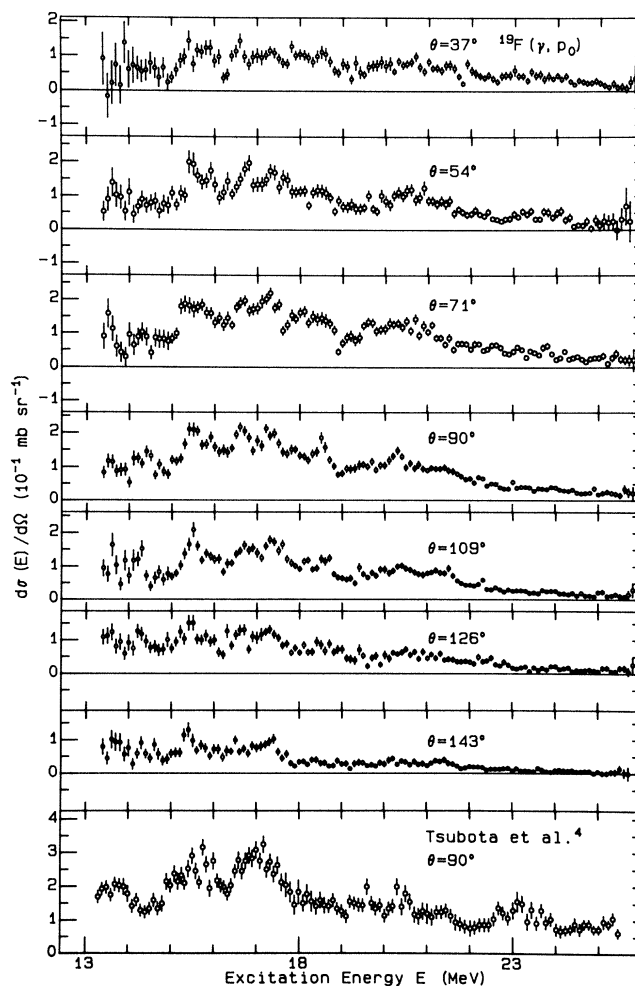


FIG. 1. The absolute differential cross sections for the $^{19}\text{F}(\gamma, p_0)$ reaction; the error bars purely represent the statistical errors. The result of Tsubota *et al.* (Ref. 4) at 90° is shown in the lower part of the figure for comparison.

II. EXPERIMENTAL PROCEDURE AND DATA ANALYSIS

Photoprotons from a thin Teflon foil (CF_2 ; 2.66 mg/cm^2), irradiated with a beam of bremsstrahlung photons produced at the 70 MeV linear electron accelerator of the Ghent University, were detected simultaneously at seven different angles θ (between 37° and 143°) using uncooled Si(Li) detectors. The experimental energy resolution, determined by the target thickness, is of the order of 100 keV for 8 MeV protons. A detailed description of the experimental setup can be found elsewhere.¹¹

Spectra were measured at bremsstrahlung end point energies varying between 15.5 and 26.0 MeV, in 0.75 MeV intervals. As the first excited state in the residual nucleus ^{18}O is located at 1.98 MeV, this small end point energy step allowed us to derive absolute differential cross sections for the (γ, p_0) reaction in a direct way. Likewise, as the second excited state in ^{18}O is located at 3.56 MeV, we could use the same peeling procedure to deduce the absolute differential (γ, p_1) cross sections as well. (For more details on the analysis procedure and the corrections applied, see Ref. 12.) The differential cross section results are shown in Figs. 1 and 2.

To these differential cross sections, a sum of Legendre

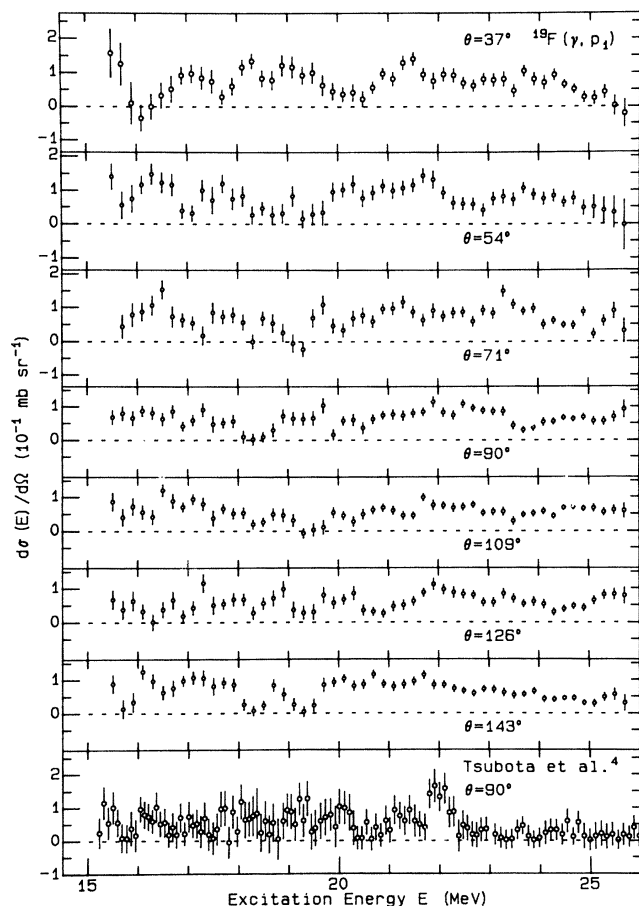


FIG. 2. The absolute differential cross sections for the $^{19}\text{F}(\gamma, p_1)$ reaction; the error bars purely represent the statistical errors. The result of Tsubota *et al.* (Ref. 4) at 90° is shown in the lower part of the figure for comparison.

polynomials was fitted:

$$\frac{d\sigma}{d\Omega}(E, \theta) = \frac{1}{4\pi} \sigma(E) \left[1 + \sum_{i=1}^n a_i(E) P_i(\cos\theta) \right].$$

The fitting was performed up to fourth order for the (γ, p_0) results, and—in view of the poorer statistics—up to second order for the (γ, p_1) data.

III. RESULTS AND DISCUSSION

A. The integrated-over-angles cross section

The integrated-over-angles (γ, p_0) cross section $\sigma(E)$ is shown in Fig. 3(a). It exhibits pronounced structure at 13.65, 14.35, 15.45, 16.70, 17.35, and 18.55 MeV excitation energy, while some indication of structure can be found at 15.85 and 17.90 MeV. The higher energy region is dominated by a broad bump centered around 20.5 MeV, with additional minor structures at 19.5, 21.3, 22.2, and 23.5 MeV. There is good agreement concerning the structure with the older (γ, p) and (e, p) measurements,^{4–8,13,14} although the amount of fine structure seen in our experiment is much larger than in the older results, due to a far better energy resolution.

The (γ, p_0) reaction has been studied for other light ($2s-1d$) nuclei such as ^{17}F (only at 90°) (Ref. 15) and ^{20}Ne (Ref. 2). The results are compared with our cross section

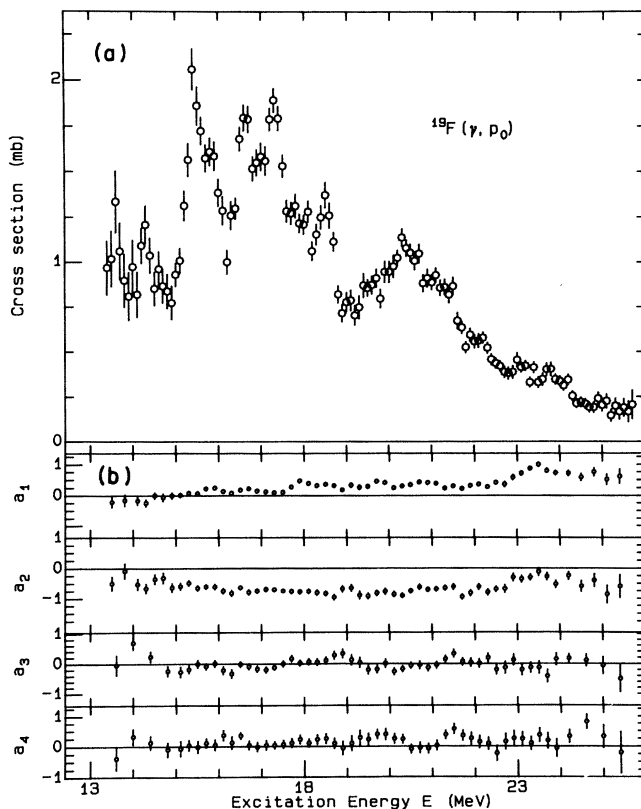


FIG. 3. (a) The over-angles-integrated $^{19}\text{F}(\gamma, p_0)$ cross section. (b) The angular distribution coefficients $a_i(E)$, $i=1, \dots, 4$, as a function of excitation energy.

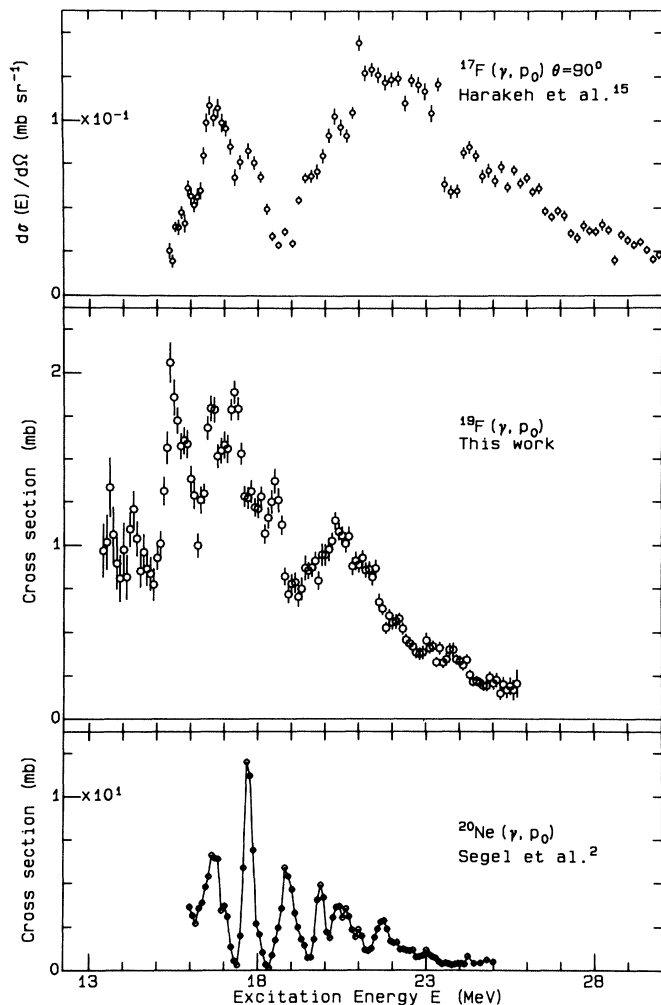


FIG. 4. The (γ, p_0) cross sections for the nuclei ^{17}F (upper), ^{19}F (middle), and ^{20}Ne (lower).

for the $^{19}\text{F}(\gamma, p_0)$ reaction in Fig. 4. One notices immediately the striking differences between these cross sections, indicating that adding one or two valence nucleons has a drastic effect on the shape of the cross section. Clearly, these valence nucleons do not behave as just "spectators," but indeed have a large influence on the location and shape of the collective dipole vibration.

Another interesting feature that emerges from Fig. 4 is the decreasing mean energy of the (γ, p_0) cross section for ^{20}Ne and ^{19}F as compared to ^{17}F . This agrees with the predictions of Neudatchin and Shevchenko on the characteristics of the configurational splitting.¹⁶ They state that the $(2s-1d)^{-1}(2p-1f)$ configurations are located at decreasing excitation energy for increasing atomic mass, and that these play a dominant role in the (γ, p_0) reaction.

The energy integrated (γ, p_0) cross section over the energy region 13.4–25.8 MeV equals (11.1 ± 0.1) MeV mb, or about 4% of the Thomas-Reiche-Kuhn (TRK) sum rule. For the 90° differential cross section, integration over the interval 13.4–25.4 MeV yields (1.22 ± 0.02) MeV mb sr^{-1} . The only comparable result is that of Tsubota *et al.*,⁴ shown in Fig. 1; their integrated cross section

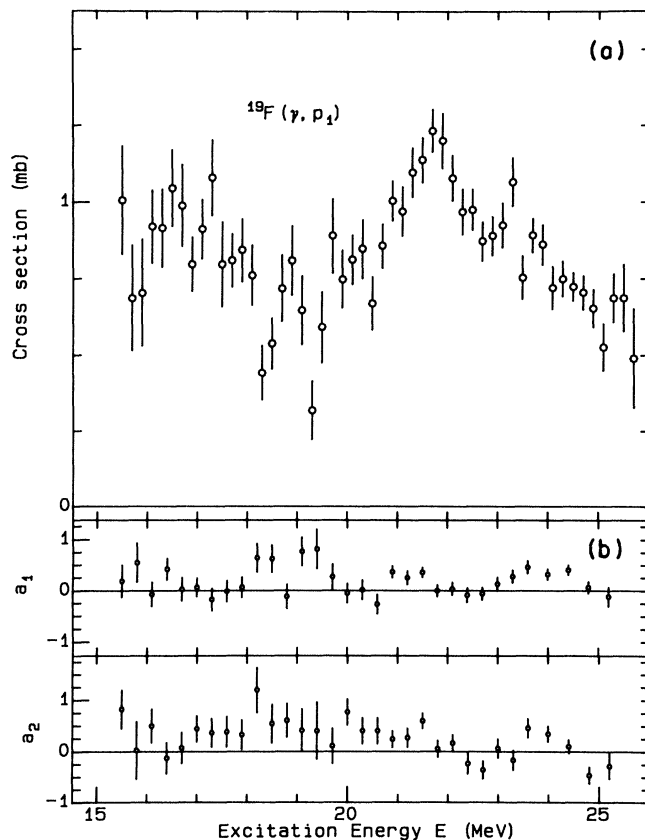


FIG. 5. (a) The over-angles-integrated $^{19}\text{F}(\gamma, p_1)$ cross section. (b) The angular distribution coefficients $a_i(E)$, $i=1,2$, as a function of excitation energy.

over the same energy region is $1.80 \text{ MeV mb sr}^{-1}$, i.e., about 50% higher than our value. We have no explanation for this discrepancy.

The integrated-over-angles (γ, p_1) cross section is shown in Fig. 5(a). Although the statistical accuracy is much poorer than in the (γ, p_0) case, one can still clearly distinguish two main bumps, at about 17.0 and 21.5 MeV excitation energy. This result shows a certain similarity with the (γ, p_0) cross section presented in Fig. 3(a), which also exhibits, apart from the fine structure, two main peaks in the cross section, centered around 17.0 and around 20.5 MeV. However, there is a marked difference in the relative magnitude of both bumps. As the ground and first excited states in the residual nucleus ^{18}O do have distinctive structures,¹⁷ this suggests that these two maxima in the cross sections are dominated by dipole states with different configurations. This difference in magnitude is therefore to be attributed to the effect of configurational splitting.

The energy integrated (γ, p_1) cross section over the region 15.4–25.8 MeV is (8.6 ± 0.2) MeV mb, again only 3% of the classical dipole sum. For the 90° differential cross section, integration over the interval 15.4–25.4 MeV yields (0.69 ± 0.03) MeV mb sr^{-1} , to be compared with the value $0.50 \text{ MeV mb sr}^{-1}$ obtained from the data of Tsubota *et al.* (shown in Fig. 2), now about 30% lower than our value.

If we compare the integrated (γ, p_0) cross section with the total (γ, p) result, which we could also derive from our experimental data (and on which we will report in a forthcoming paper), it turns out that the (γ, p_0) channel contributes only 7% to the (γ, p) reaction. This is in marked contrast to the large ground state contribution (about 40%) in the (γ, p) reaction of the even-even nuclei ^{16}O (Refs. 1 and 19) and ^{20}Ne (Refs. 2 and 20). The low value for the $^{19}\text{F}(\gamma, p_0)$ and (γ, p_1) cross sections can be accounted for in a semidirect reaction model, since the proton pickup spectroscopic factors for the ^{18}O levels¹⁷ show a much smaller overlap with the ^{19}F ground state for the states which have a $(2s-1d)$ proton hole with respect to ^{19}F (such as the ground and first excited state of ^{18}O) than for the $1p$ hole states.

B. The angular distributions

The angular distribution coefficients a_i ($i=1-4$) for the (γ, p_0) reaction are shown in Fig. 3(b). The asymmetry coefficient a_1 rises slowly from zero at low energies to a maximum of 0.75 at 23.5 MeV, which indicates important interference effects at high energy. The other asymmetry coefficient a_3 is very small, but on the average nonzero and negative, again indicating interference between multipoles of different polarity. The anisotropy coefficient a_2 shows some structure but remains negative, with a minimum value close to -1.0 in the central part of the energy range, and with maxima, approaching zero, at 14.0 and 23.5 MeV, indicating possibly a higher $E2$ fraction at these energies. Finally, the $E2$ coefficient a_4 is small, but remains positive over almost the entire region; again, this indicates a nonnegligible $E2$ contribution over the whole energy interval. Asymmetric angular distributions have already been measured, over a limited energy range, in earlier (γ, p) experiments,⁵⁻⁸ and were in some cases related to $E2$ interference effects.^{5,8}

A quantitative derivation of the $E2$ contribution from angular distribution measurements is often rather speculative, due to the approximations that have to be made to reduce the number of electromagnetic multipole transition matrix elements (see, e.g., Ref. 12). From the above considerations, it is clear that in this case certainly no $E2$ matrix elements can be neglected. However, we felt that we could disregard all $M1$ contributions, as the $M1$ strength is believed to be concentrated around $35A^{-1/3}$ MeV excitation energy in light nuclei,²¹ that is, around 13 MeV in ^{19}F . Thus, the above approximation may be incorrect at the lowest energies considered.

Taking then only $E1$ and $E2$ contributions into account, there are only four possible transition matrix elements in this reaction.¹⁸ However, as the three phase differences between the complex matrix elements also have to be determined, we have seven unknowns and the problem is underdefined. To reduce the number of unknowns, we assume that the phases are independent of the angular momentum j of the intermediate state, that is, we assume no phase difference between the $p_{1/2}$ and $p_{3/2}$ $E1$ matrix elements (describing $E1$ transitions to the $\frac{1}{2}^-$ and $\frac{3}{2}^-$ state, followed by p -wave or $l=1$ proton emission, in the channel spin formalism), or between the $d_{3/2}$ and $d_{5/2}$

$E2$ matrix elements (describing $E2$ transitions to $\frac{3}{2}^+$ and $\frac{5}{2}^+$ states, followed by d -wave or $l=2$ proton emission). This approach is based on the fact that for radiative capture reactions, the relative phase is given by the following:²²

$$\begin{aligned} \phi_l - \phi_{l'} = & -\arctan[F_l(R)/G_l(R)] + \eta_l \\ & + \arctan[F_{l'}(R)/G_{l'}(R)] - \eta_{l'} + n\pi \end{aligned} \quad (1)$$

under the assumption that the target nucleus can be described by the model of a hard-core scatterer with a Coulomb field, and that there is no interference between various resonances.²³ The functions F_l and G_l are the regular and irregular Coulomb functions, while η_l is the Coulomb phase shift. This expression for the phase differences has been used several times in the analysis of capture angular distributions.^{2,24-25} However, we do not rely on its explicit form; all that matters here is that

$$\phi_l - \phi_{l'} = n\pi \text{ if } l=l',$$

the validity of which has been confirmed, apart from some minor deviations due to spin orbit coupling, in a recent $^{30}\text{Si}(\bar{p}, \gamma_0)^{31}\text{P}$ experiment.²⁶

As only one phase difference

$$\phi = (\phi_{l=1} - \phi_{l'=2}),$$

is left to be determined, the set of five equations suffices to calculate the five unknowns. The equations can be written as the following:¹⁸

$$\begin{aligned} 1 &= p_{1/2}^2 + 2p_{3/2}^2 + 2d_{3/2}^2 + 3d_{5/2}^2, \\ a_1 &= 2\sqrt{3}(p_{1/2}d_{3/2} + \frac{9}{5}p_{3/2}d_{5/2} \\ &\quad + \frac{1}{5}p_{3/2}d_{3/2}) \cos\phi, \\ a_2 &= -p_{3/2}^2 - 2p_{1/2}p_{3/2} + d_{3/2}^2 + \frac{12}{7}d_{5/2}^2 \\ &\quad + \frac{6}{7}d_{3/2}d_{5/2}, \\ a_3 &= -2\sqrt{3}(p_{1/2}d_{5/2} + \frac{4}{5}p_{3/2}d_{5/2} \\ &\quad + \frac{6}{5}p_{3/2}d_{3/2}) \cos\phi, \\ a_4 &= -\frac{12}{7}d_{5/2}^2 - \frac{48}{7}d_{3/2}d_{5/2}. \end{aligned}$$

The short-hand notation x_j stands for $(-1)^n |x_j|$, where x_j is the corresponding complex matrix element, and the sign ambiguity comes from the last term in Eq. (1).

Solving this set of equations is straightforward, and leads to two possible results for the $E2$ fraction in the (γ, p_0) cross section. Without additional information, there is no way to decide which is the correct one. However, as can be seen from Fig. 6(a), the two results are very close to each other. The overall shape agrees quite well with our qualitative considerations: The $E2$ contribution shows a minimum around 19 MeV, and maxima around 14 and 23.5 MeV.

The magnitude of the $E2$ contribution might seem somewhat unrealistic, but one should bear in mind that polarized proton capture experiments have also revealed considerable $E2$ strength in the neighboring nuclei ^{16}O and ^{20}Ne (Ref. 21). This strength would, however, prob-

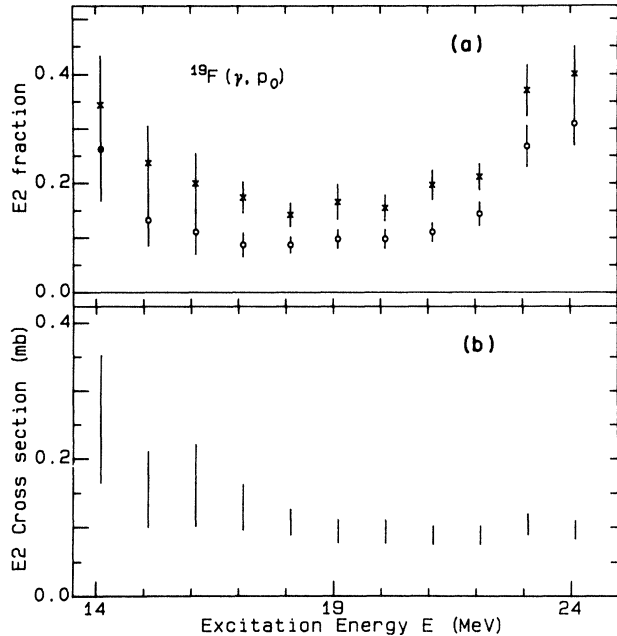


FIG. 6. (a) The calculated “low” (open circles) and “high” (crosses) solution for the $E2$ fraction in the $^{19}\text{F}(\gamma, p_0)$ cross section (see the text). (b) The (γ, p_0) $E2$ cross section extracted from the “low” solution.

ably be mostly of isovector nature, as it is found at higher excitation energies than the strength in α capture or hadron scattering experiments.²⁷ Our results are further supported by the agreement of the $E2$ strength distribution with the expectations for light nuclei:²⁸ no resonance behavior, but a broad, structured distribution, situated below the predicted excitation energy ($63A^{-1/3}$ MeV). In fact, these are the same characteristics as those of the $E1$ giant resonance in light nuclei²⁸ (and possibly of all giant resonances). Therefore, one would also expect to find at least an indication of deformation splitting in the giant quadrupole resonance (GQR), since it was suggested to be present in the giant dipole resonance of ^{19}F (Refs. 29 and 30). Such a deformation splitting has been predicted for the similarly deformed nucleus ^{20}Ne (Refs. 31 and 32) and was found experimentally.^{33,34} We therefore believe that the observed splitting in the (γ, p_0) $E2$ contribution is related to the deformation of the ^{19}F nucleus, especially as the splitting is very similar to the one predicted and observed in ^{20}Ne (see Fig. 7).

Taking all these arguments into consideration, we feel that we can be rather confident of our $E2$ results, at least as far as the strength distribution is concerned. From the

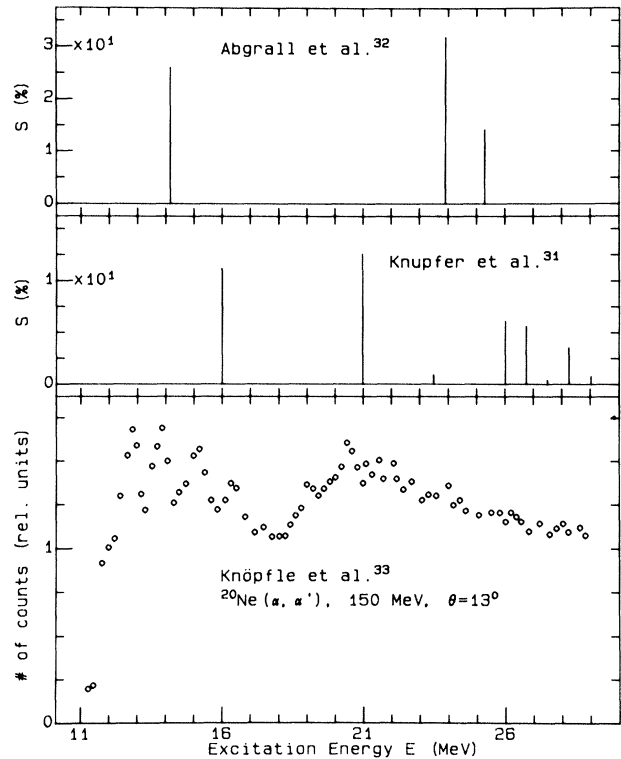


FIG. 7. Theoretically predicted $E2$ distributions for ^{20}Ne compared to a measured (α, α') spectrum, shown in the lower part of the figure.

lowest solution, we calculated the $E2$ cross section, shown in Fig. 6(b), and the contribution to the $E2$ energy-weighted sum rule. As we have mentioned, the detected $E2$ strength is probably partly isoscalar and partly isovector. Therefore, a comparison has to be made with the total energy-weighted sum rule. In Table I, this is done for the smallest solution, as well as for the “minimum” $E2$ cross section, calculated independently from the a_4 coefficient only.¹² The agreement between both results suggests their reliability.

It turns out that the (γ, p_0) $E2$ cross section exhausts $(37 \pm 7)\%$ of the total $E2$ energy-weighted sum rule. This value is extremely high, and should be referred to with some care. In fact, we do believe that our $E2$ cross section may be overestimated, due to the influence of the a_4 coefficient, of which the statistical significance is not beyond doubt.¹² However, it could be that the extremely large $E2$ contribution results from the neglect of possible $M1$ strength. As this strength is supposed to be located around 13 MeV, it might contribute in the low energy re-

TABLE I. The contribution of the $^{19}\text{F}(\gamma, p_0)$ $E2$ cross section, deduced from the present experiment, to the EWSR value which is equal to $6.709 (\Delta T=0) + 7.454 (\Delta T=1) \mu\text{b}/\text{MeV}$.

$E2$ solution	σ_{-2} ($\mu\text{b MeV}^{-1}$)	Sum rule fraction		
		$\Delta T=0$	$\Delta T=1$	$(\Delta T=0)+(\Delta T=1)$
“Low”	5.28 ± 0.94	0.79 ± 0.14	0.71 ± 0.13	0.37 ± 0.07
“Min”	4.72 ± 2.36	0.70 ± 0.35	0.63 ± 0.32	0.33 ± 0.17

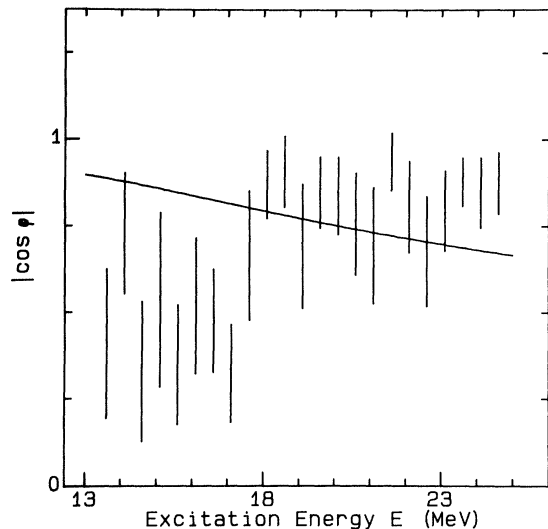


FIG. 8. The absolute value of $\cos\phi$, wherein ϕ is derived from Eq. (1) (full line), and from the angular distribution coefficients (data points).

gion of our results. Moreover, if we assume the $M1$ giant resonance to show the same characteristics as $E1$ and $E2$, it might be spread out over an energy interval of several MeV, thus contributing possibly up to 16 MeV or even higher. Since it is in this area that the $E2$ cross section contributes mostly to the energy-weighted sum rule, any small $M1$ fraction would reduce the sum rule value significantly. It is worthwhile mentioning here that a comparison between the phase difference ϕ derived from the angular distribution coefficients, and the theoretical value of Eq. (1), is satisfactory in the higher energy region, but rather meaningless below 18 MeV (Fig. 8). This again might be an indication of unjustly neglected ($M1$) matrix elements.

The angular distribution coefficients a_1 and a_2 for the (γ, p_1) reaction are shown in Fig. 5(b). As the residual nucleus is left in a 2^+ state, the number of possible electromagnetic multipole transition matrix elements is much larger, and they cannot be determined unambiguously from our data. The a_1 coefficient is definitely nonzero and almost everywhere positive, indicating interference ef-

fects between states of opposite parity. The a_2 coefficient again is nonzero and, in contrast to the a_2 coefficient for (γ, p_0) , mainly positive.

IV. CONCLUSIONS

We have measured the absolute ground and first excited state photoproton cross sections and angular distributions for ^{19}F in the energy region between 13.4 and 25.8 MeV, using a bremsstrahlung photon beam. Our energy resolution was better than in any of the older (γ, p) measurements, allowing us to observe more detailed fine structure.

Comparison with neighboring nuclei revealed the influence of the valence nucleons, and confirmed the predictions of Neudatchin and Shevchenko on the configurational splitting.¹⁶ Furthermore, our data confirm the trend of small (γ, p_0) cross sections for odd- Z nuclei, first noticed by Shoda.³ These low (γ, p_0) and (γ, p_1) cross sections are in our opinion simply the reflection of the small overlap between the ground state of the target nucleus and the ground and first excited states of the residual nucleus.

Although they show some similarities, the (γ, p_0) and (γ, p_1) cross sections are distinctly different in the relative magnitude of their structures. This was not to be expected if they had originated from dipole states with the same configurations. We believe that their differences are therefore a manifestation of configurational splitting effects.

The observed angular distributions indicate the presence of other than $E1$ excitations over the entire energy region. A quantitative analysis of the (γ, p_0) angular distribution coefficients, neglecting $M1$ contributions, leads to an estimated $E2$ cross section exhausting about 37% of the total (isoscalar plus isovector) $E2$ energy-weighted sum rule. However, the inclusion of $M1$ excitations can significantly lower this value.

ACKNOWLEDGMENTS

We thank Professor A. J. Deruytter for his interest during the course of this work. We are especially grateful to the linac crew for the operation of the linear accelerator. We also acknowledge the financial support lent by the Interuniversity Institute for Nuclear Sciences (IIKW) and the National Foundation for Scientific Research (NFWO), Brussels.

¹W. J. O'Connell and S. S. Hanna, Phys. Rev. C **17**, 892 (1978).

²R. E. Segel, Z. Vager, L. Meyer-Schützmeister, P. P. Singh, and R. G. Allas, Nucl. Phys. **A93**, 31 (1967); J. R. Calarco, P. M. Kurjan, G. A. Fisher, and S. S. Hanna, Phys. Lett. **92B**, 67 (1980).

³K. Shoda, Nucl. Phys. **72**, 305 (1965).

⁴H. Tsubota, N. Kawamura, S. Oikawa, and J. Uegaki, J. Phys. Soc. Jpn. **38**, 299 (1975).

⁵B. Forkman and I. Wahlström, Ark. Fys. **18**, 339 (1960).

⁶W. R. Dodge and W. C. Barber, Phys. Rev. **127**, 1746 (1962).

⁷E. Braun, Z. Phys. **166**, 62 (1962).

⁸S. Seki, M. Yamanouchi, and M. Miwa, J. Phys. Soc. Jpn. **19**, 1999 (1964).

⁹K. W. Schmid and G. Do Dang, Phys. Lett. **66B**, 5 (1977); Phys. Rev. C **15**, 1515 (1977); **18**, 1003 (1978).

¹⁰N. K. Sherman, K. H. Lokan, and R. W. Gellie, Can. J. Phys. **54**, 1178 (1976).

¹¹R. Carchon, R. Van de Vyver, H. Ferdinande, J. Devos, and E. Van Camp, Phys. Rev. C **14**, 456 (1976).

¹²E. Van Camp, R. Van de Vyver, H. Ferdinande, E. Kerkhove, R. Carchon, and J. Devos, Phys. Rev. C **22**, 2396 (1980).

¹³K. M. Murray and W. L. Bendel, Phys. Rev. **132**, 1134 (1963).

¹⁴K. Abe, E. Tanaka, N. Kawamura, M. Kanazawa, and N. Mutowo, J. Phys. Soc. Jpn. **25**, 1507 (1968).

¹⁵M. N. Harakeh, P. Paul, and P. Gorodetzky, Phys. Rev. C **11**, 1008 (1975).

¹⁶V. G. Neudatchin and V. G. Shevchenko, Phys. Lett. **12**, 18 (1964).

¹⁷G. T. Kaschl, G. J. Wagner, G. Mairle, U. Schmidt-Rohr, and

- P. Turek, Nucl. Phys. **A155**, 417 (1970).
- ¹⁸R. W. Carr and J. E. E. Baglin, Nucl. Data Tables **A10**, 143 (1971).
- ¹⁹J. G. Woodworth, K. G. McNeill, J. W. Jury, R. A. Alvarez, B. L. Berman, D. D. Faul, and P. Meyer, Phys. Rev. C **19**, 1667 (1979).
- ²⁰P. D. Allen, E. G. Muirhead, and D. V. Webb, Nucl. Phys. **A357**, 171 (1981).
- ²¹S. S. Hanna, *Lecture Notes in Physics*, Vol. 61, edited by S. Costa and C. Schaerf (Springer, Berlin, 1977), p. 275.
- ²²H. J. Rose and D. M. Brink, Rev. Mod. Phys. **39**, 306 (1967).
- ²³R. J. Holt, R. M. Laszewski, H. E. Jackson, J. E. Monahan, and J. R. Specht, Phys. Rev. C **21**, 1699 (1980).
- ²⁴R. G. Allas, S. S. Hanna, L. Meyer-Schützmeister, and R. E. Segel, Nucl. Phys. **58**, 122 (1964).
- ²⁵E. D. Earle and N. W. Tanner, Nucl. Phys. **A95**, 241 (1967).
- ²⁶C. P. Cameron, R. D. Ledford, M. Potokar, D. G. Rickel, N. R. Roberson, H. R. Weller, and D. R. Tilley, Phys. Rev. C **22**, 397 (1980).
- ²⁷S. S. Hanna, Comments Nucl. Part. Phys. **11**, 79 (1983).
- ²⁸J. Speth and A. Van der Woude, Rep. Prog. Phys. **44**, 719 (1981).
- ²⁹J. D. King, R. N. H. Haslam, and W. J. McDonald, Can. J. Phys. **38**, 1069 (1960).
- ³⁰G. Baciú, D. Catană, C. Deberth, and I. Răileanu, Rev. Roum. Phys. **12**, 385 (1967).
- ³¹W. Knüpfer, K. Gnauss, and M. G. Huber, Phys. Lett. **66B**, 305 (1977).
- ³²Y. Abgrall, B. Morand, E. Caurier, and B. Grammaticos, Phys. Rev. Lett. **39**, 922 (1977).
- ³³K. T. Knöpfle, G. J. Wagner, A. Kiss, M. Rogge, and C. Mayer-Böricke, Phys. Lett. **64B**, 263 (1976).
- ³⁴Z. M. Szalata, K. Itoh, G. A. Peterson, J. Flanz, S. P. Fivozinsky, F. J. Kline, J. W. Lightbody, Jr., X. K. Maruyama, and S. Penner, Phys. Rev. C **17**, 435 (1978).